

## Article

# Uniaxial-Pressure-Induced Release of Magnetic Frustration in a Triangular Lattice Antiferromagnet YbCuGe

Kazunori Umeo <sup>1,\*</sup>, Daichi Watanabe <sup>2</sup>, Koji Araki <sup>3</sup>, Kenichi Katoh <sup>3</sup> and Toshiro Takabatake <sup>4</sup>

<sup>1</sup> Department of Low Temperature Experiment, Integrated Experimental Support/Research Division, N-BARD, Hiroshima University, Higashi-Hiroshima 739-8526, Japan

<sup>2</sup> Department of Quantum Matter, AdSM, Hiroshima University, Higashi-Hiroshima 739-8530, Japan; gaia12255221aiag@gmail.com

<sup>3</sup> Department of Applied Physics, National Defense Academy, Yokosuka, Kanagawa 239-8686, Japan; araki@nda.ac.jp (K.A.); katok@nda.ac.jp (K.K.)

<sup>4</sup> Graduate School of Advanced Science and Engineering, Hiroshima University, Higashi-Hiroshima 739-8530, Japan; takaba@hiroshima-u.ac.jp

\* Correspondence: kumeo@hiroshima-u.ac.jp

**Abstract:** We have studied the effect of geometrical frustration on the antiferromagnetic order in the Yb-based triangular lattice compound YbCuGe below  $T_N = 4.2$  K by the measurements of magnetization and specific heat under hydrostatic and uniaxial pressures. By applying hydrostatic pressure  $P$  up to 1.34 GPa,  $T_N$  hardly changes. By contrast,  $T_N$  increases as  $P$  is applied along the hexagonal  $a$  axis, while  $T_N$  decreases by the application of  $P$  along the  $c$  axis. The increase of  $T_N$  only for  $P \parallel a$  suggests the release of the frustration inherent in the triangular lattice of Yb ions of this compound.

**Keywords:** uniaxial pressure; antiferromagnetic order; magnetic frustration; Yb compound; magnetization; specific heat



**Citation:** Umeo, K.; Watanabe, D.; Araki, K.; Katoh, K.; Takabatake, T. Uniaxial-Pressure-Induced Release of Magnetic Frustration in a Triangular Lattice Antiferromagnet YbCuGe. *Metals* **2021**, *11*, 30. <https://dx.doi.org/10.3390/met11010030>

Received: 26 November 2020

Accepted: 24 December 2020

Published: 25 December 2020

**Publisher's Note:** MDPI stays neutral with regard to jurisdictional claims in published maps and institutional affiliations.



**Copyright:** © 2020 by the authors. Licensee MDPI, Basel, Switzerland. This article is an open access article distributed under the terms and conditions of the Creative Commons Attribution (CC BY) license (<https://creativecommons.org/licenses/by/4.0/>).

## 1. Introduction

Cerium (Ce)-based and Ytterbium (Yb)-based intermetallic compounds have a great deal of interest in the field of magnetism because they exhibit a variety of physical behaviors, such as an anomalous magnetic ordering, superconductivity, and non-Fermi-liquid behavior due to the competition between the Kondo effect and the Ruderman-Kittel-Kasuya-Yosida (RKKY) interaction [1,2]. The competition can be controlled easily by applying pressure. In fact, such unusual behaviors have been realized in many of Ce and Yb compounds under pressure [2–6].

On the other hand, magnetic properties of compounds with geometrically frustrated lattices, such as triangular, honeycomb, kagome, and pyrochlore lattices, have received considerable attention from both theorists and experimentalists [7,8]. The geometrical frustrations give rise to a number of unusual behaviors, such as suppression of magnetic ordering temperatures, multiple-phase transitions, complex magnetic structures, and spin liquid states [7,8]. In rare-earth-based intermetallic compounds with frustrated lattices, the long-range nature of the RKKY interaction has been believed to overcome the effect of frustration. However, the interplay among frustrated anisotropic exchange interactions, crystalline electric field (CEF) anisotropy, and Kondo effect arises the partial disordered magnetic state, multiple-phase transition, and unusual heavy-fermion state in Ce-and Yb compounds with the quasikagome lattices, CePdAl [9], CeRhSn [10,11], CeIrSn [12], and YbAgGe [13] as well as that with the honeycomb lattice CePt<sub>6</sub>Al<sub>3</sub> [14]. For example, in CePdAl below  $T_N = 2.7$  K, one-third of Ce ions remain in a paramagnetic state due to the geometrical frustration of the quasikagome lattice [9]. Another example is a heavy-fermion compound CePt<sub>6</sub>Al<sub>3</sub> in which Ce atoms form a honeycomb lattice in a trigonal basal plane [13]. Theoretically, a quantum spin liquid state is expected to be realized in

the stuffed honeycomb lattice that interpolates between the triangular and honeycomb lattices [15,16].

We focus on YbCuGe as a candidate of a frustrated Yb-based intermetallic compound. This compound crystallizes in the hexagonal NdPtSb-type structure in which Yb atoms form a triangular lattice in the  $c$  plane, as shown in Figure 1 [17]. The magnetic susceptibility  $\chi = M/B$  above 100 K for both  $B \parallel c$  and  $B \parallel a$  follows the Curie-Weiss law expected for the trivalent Yb ion [18]. The easy magnetization direction along the  $c$  axis can be explained by the CEF effect on a single Yb ion. The broad maximum of the magnetic specific heat at 50 K is reproduced as a Schottky anomaly by the CEF model [18]. This compound shows an antiferromagnetic order at  $T_N = 4.2$  K, where a sharp peak appears in the specific heat  $C(T)$  and a shoulder in  $\chi_a$  and a hump in  $\chi_c$ . The Sommerfeld coefficient is as small as 5.2 mJ/K<sup>2</sup>mol [18], suggesting the Kondo effect to be very weak. However,  $C(T)$  shows a broad tail above  $T_N$  and the magnetic entropy at  $T_N$  is 28% of  $R\ln 2$ . These results hint to the effect of a magnetic frustration in the triangular lattice of trivalent Yb ions in this compound. In this study, to reveal the magnetic frustration, we have measured the magnetic susceptibility and specific heat under uniaxial and hydrostatic pressures  $P$ . When  $P$  is applied along the  $a$  axis, the magnetic frustration should be released due to the distortion of the regular triangle of Yb ions in the  $c$  plane, while the frustration remains under the uniaxial pressure of  $P \parallel c$  and hydrostatic pressure, which keep the triangle equilateral. The comparison of the results under the uniaxial and hydrostatic pressures will be presented and discussed.

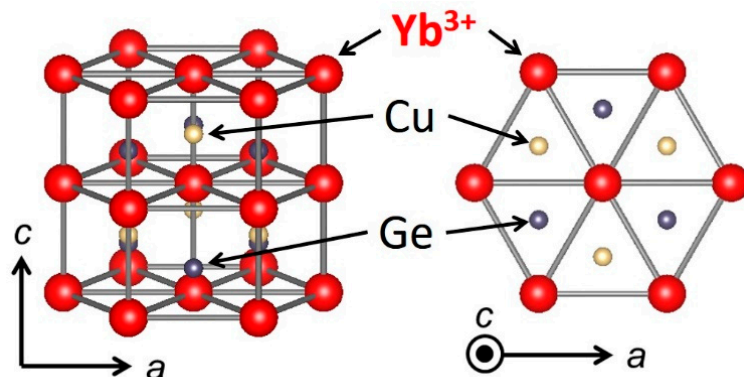


**Figure 1.** Crystal structure of YbCuGe with a triangular lattice of Yb atoms in the  $c$  plane of the hexagonal NdPtSb-type structure.

## 2. Experimental Procedures

Single-crystalline samples of YbCuGe were prepared by the Bridgman method in a sealed tungsten crucible, as reported previously [18]. The crystal structure of YbCuGe has been confirmed by X-ray diffraction measurements using a single crystal and powder samples, as reported in the previous paper [17]. The X-ray powder diffraction measurement on the powdered single crystals detected no impurity phases [18]. The crystals were oriented by the Laue method and shaped by the spark erosion for the measurements of magnetic susceptibility  $\chi = M/B$  and specific heat  $C$ . At hydrostatic and uniaxial pressures,  $\chi$  was measured by using a commercial superconducting quantum interference device magnetometer (Quantum Design, MPMS, San Diego, CA, USA). For hydrostatic pressures up to 1.34 GPa, a piston-cylinder pressure cell made of NiCrAl alloy and Daphne oil 7373 as a pressure transmitting medium were used. For uniaxial pressure of the configurations  $P \parallel B$  and  $P \perp B$ , two type of pressure cells were constructed [19]. Uniaxial pressures were applied on a sample plate of 0.4–0.7 mm in thickness by a homemade pressure cell made of ZrO<sub>2</sub>. The applied pressure was determined by measuring the superconducting transition temperature  $T_c$  of a piece of tin [20], which was placed at the lower part of the pressure cell.

The C under uniaxial pressures was measured up to 0.45 GPa by using a home-made ac calorimeter in the temperature range of 0.5 to 10 K [21]. Figure 2 shows the pressure cell and sample setting for the ac calorimeter under uniaxial pressures [22]. Thereby, we used disk-shape samples of 2 mm in diameter and 0.5 mm in thickness. Two RuO<sub>2</sub> chip resistors as a thermometer and a heater, respectively, were mounted on the fringe of the Cu-Be plate. To thermally isolate the Cu-Be plate and sample from the ZrO<sub>2</sub> piston, diamond powder of a 0.25-μm diameter was placed on the top of the piston. The sample of YbCuGe and the sample of In metal used as a pressure gauge are placed in the cell in the vertical direction, as shown in Figure 2. Therefore, the pressure for the sample should be equal to that for the In metal. The pressure for the In metal was determined from the pressure dependence of the superconducting transition temperature of In metal [23]. The superconducting transition was measured by the diamagnetic signal of ac magnetic susceptibility.

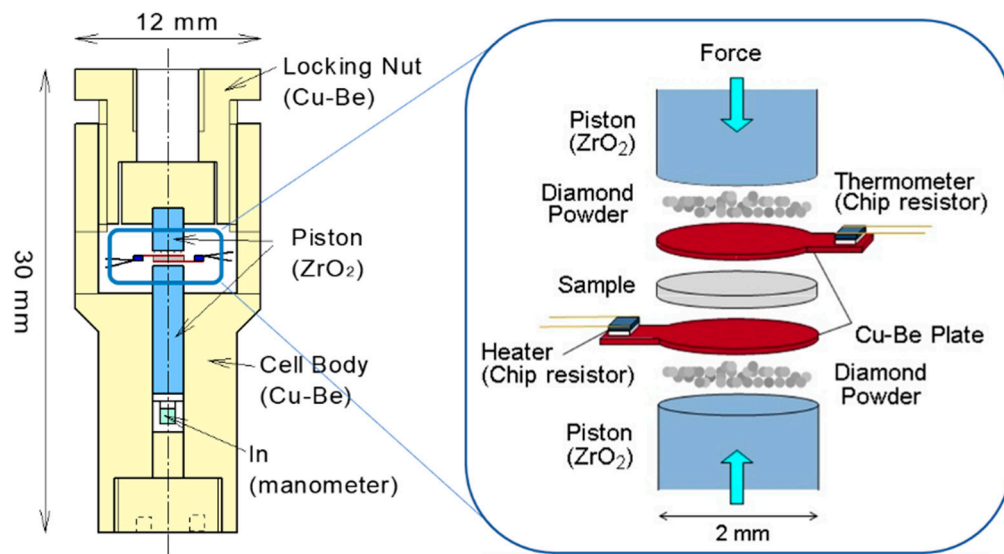
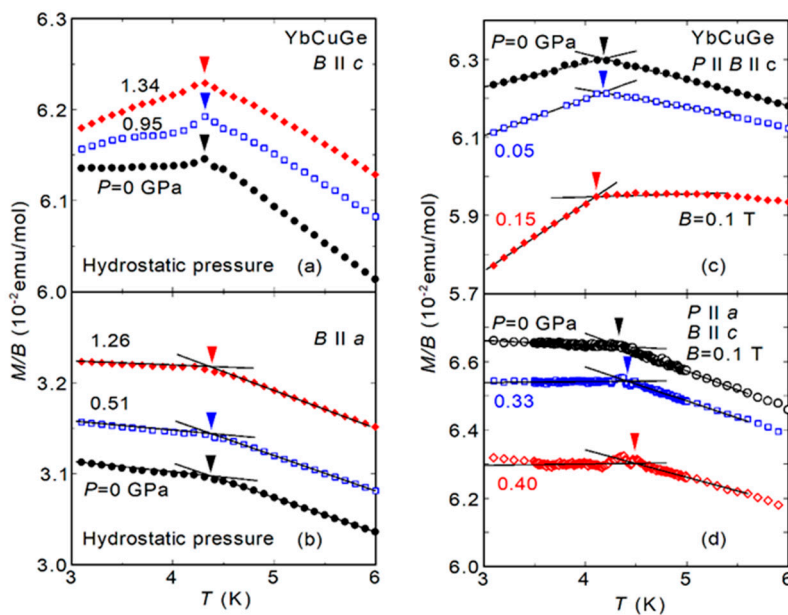


**Figure 2.** Schematic drawing of the ac calorimeter under uniaxial pressure.

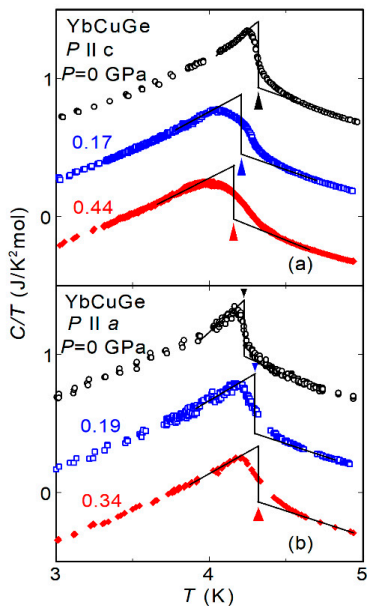
### 3. Results and Discussion

Figure 3 shows the temperature dependence of  $\chi = M/B$  of YbCuGe under hydrostatic and uniaxial pressures. The maximal temperature of  $\chi$  ( $T$ ) for Figure 3a was taken as the Néel temperature  $T_N$ . The value of  $T_N$  for Figure 3b-d was taken as the temperature where the two lines extrapolated from above and below the kink intersect. For hydrostatic pressure,  $T_N$  hardly changes, while  $T_N$  under uniaxial pressure displays opposite variations, a decrease for  $P \parallel c$ , and an increase for  $P \parallel a$ . The increase of  $T_N$  only for  $P \parallel a$  suggests the release of the frustration inherent in the triangular lattice of Yb ions of this compound. The variations of  $T_N(P)/T_N(0)$  for hydrostatic and uniaxial pressures are plotted in Figure 5, which will be discussed later. Note that the value of  $\chi$  increases with increasing hydrostatic pressure, while  $\chi$  decreases for uniaxial pressures both  $P \parallel c$  and  $P \parallel a$ .

To confirm the opposite variations of  $T_N$  for  $P \parallel c$  and  $P \parallel a$ , we have measured the specific heat under uniaxial pressures. As shown in Figure 4a, with increasing  $P \parallel c$ , the peak of the specific heat C divided by temperature  $C/T$  becomes broader and the peak temperature shifts to a lower temperature range. For  $P \parallel a$  in Figure 4b, on the contrary, the peak temperature shifts to a higher temperature range. The  $T_N$  was determined by considering the entropy balance above and below  $T_N$ , as shown in Figure 4.



**Figure 3.** Temperature dependence of the magnetic susceptibility  $M/B$  of YbCuGe under hydrostatic pressures (a,b) and uniaxial pressures (c,d). The data at 0.33 GPa are shifted downward by  $0.1 \times 10^{-2}$  emu/mol to avoid the overlap with the data for 0 GPa. The arrows indicate the antiferromagnetic ordering temperature  $T_N$ , where  $T_N$  in (b-d) is taken as the intersection of the two lines above and below  $T_N$ .



**Figure 4.** Temperature dependence of the specific heat divided by temperature  $C/T$  of YbCuGe under uniaxial pressures applied along the  $c$  axis (a) and  $a$  axis (b). The arrows indicate the antiferromagnetic ordering temperature  $T_N$ . The data sets at various pressures are shifted downward by  $0.5 J/K^2\text{mol}$  for clarity.

The uniaxial pressure dependences of  $T_N$  are compared in Figure 5 together with that for hydrostatic pressure. We plot the values of  $T_N$  normalized by the value at  $P = 0$  because  $T_N$  ( $P = 0$ ) depends slightly on the samples. Now, we will discuss the pressure dependence of  $T_N$  in terms of the change only in the exchange interaction  $J$  between Yb ions with pressures. Thereby, a change in the Kondo effect is neglected because the Kondo effect is

sufficiently weak even at an ambient pressure, as mentioned above. At first, under both hydrostatic pressure and  $P \parallel c$ , the equilateral nature of the triangle should hold. However,  $T_N$  for hydrostatic pressure hardly changes while  $T_N$  decreases for  $P \parallel c$ . Under hydrostatic pressure, the shrinkage along both  $a$  and  $c$  axes may enhance both  $J_a$  along the  $a$ -axis and  $J_c$  along the  $c$ -axis as manifested in the increment of  $\chi$ , which is shown in Figure 3a,b. However, the enhancement of  $J_a$  may strengthen the magnetic frustration effect. Therefore, the unchanged  $T_N$  for the hydrostatic pressure may result from the compensation between the two effects of enhanced exchange interaction and strengthened magnetic frustration. On the other hand, for  $P \parallel c$ , the lattice expands along the  $a$ -axis, as shown in the inset of Figure 5, while it shrinks along the  $c$ -axis. Therefore, it would be expected that  $J_a$  decreases while  $J_c$  increases. However, the decrease of the value of  $\chi$  as shown in Figure 3c suggests that the net value of  $J$  decreases with increasing  $P \parallel c$ . Therefore, the suppression of  $J$  may lead to the decrease in  $T_N$ .

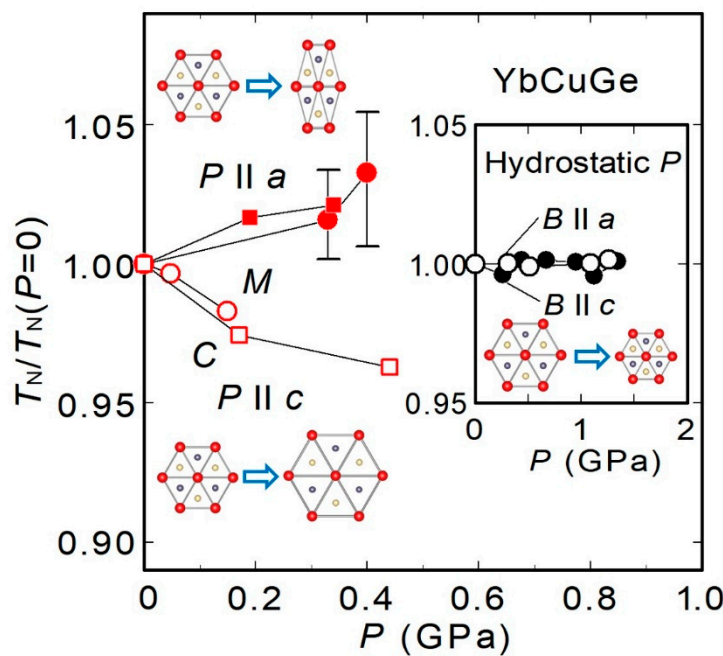


**Figure 5.** Uniaxial pressure dependence of the antiferromagnetic ordering temperature  $T_N$  of YbCuGe, where the data of  $T_N$  are normalized by the value at ambient pressure. The inset shows the hydrostatic pressure dependence of  $T_N$ . The circles and squares denote the data obtained from the specific heat  $C$  and magnetization  $M$  measurements, respectively. The schematic changes in the triangular configuration in the hexagonal  $c$  plane under uniaxial and hydrostatic pressures are drawn in the main frame and inset, respectively. The balls in red, yellow, and black denote the Yb, Cu, and Ge atoms, respectively.

For  $P \parallel a$ , the regular triangle in the  $c$  plane would be distorted, as shown in the inset of Figure 5. In this case, the Yb-Yb distance parallel to the pressure decreases but that nonparallel to the pressure in the  $c$  plane increases. This makes it difficult to guess how the value of  $J_a$  would change. However, for  $P \parallel a$ , the value of  $\chi$  decreases for  $B \parallel c$  (Figure 3d) as well as for  $B \parallel a$  (not shown). This fact suggests that the net value of  $J_a$  decreases for  $P \parallel a$ . Nevertheless,  $T_N$  for  $P \parallel a$  increases, which should result from the release of the magnetic frustration in the triangular lattice of this compound. A similar release of the frustration under uniaxial pressure has been found in an Fe-based triangular lattice system [24]. To confirm this conjecture on YbCuGe, neutron diffraction measurements under pressures are highly desirable.

#### 4. Conclusions

To reveal the effect of magnetic frustration in the Yb-triangular-lattice antiferromagnet YbCuGe with  $T_N = 4.2$  K, we have studied the response of the magnetic susceptibility and specific heat to uniaxial and hydrostatic pressures. It is found that  $T_N$  increases by the application of  $P$  only along the  $a$ -axis, which violates the symmetry of the triangular lattice. This finding indicates the release of the frustration inherent in the triangular lattice of Yb ions of this compound.

**Author Contributions:** Conceptualization, K.U. and K.K. Methodology, K.U. Validation, K.U., D.W., K.K., and T.T. Formal analysis, K.U. and D.W. Investigation, K.U. and D.W. Resources, K.U., D.W., K.A., and K.K. Data curation, K.U. and D.W. Writing—original draft preparation, K.U. Writing—review and editing, T.T. Visualization, K.U. and D.W. Supervision, K.U. Project administration, K.U., K.K., and T.T. Funding acquisition, K.U. and T.T. All authors have read and agreed to the published version of the manuscript.

**Funding:** This work was partly supported by Japan Society for the Promotion of Science KAKENHI Grants Nos. JP25400375 and JP17K05545.

**Institutional Review Board Statement:** Not applicable.

**Informed Consent Statement:** Not applicable.

**Acknowledgments:** We acknowledge valuable discussions with T. Onimaru. The magnetic susceptibility measurement under pressures was performed at N-BARD, Hiroshima University.

**Conflicts of Interest:** The authors declare no conflict of interest.

#### References

1. Doniach, S. The Kondo lattice and weak antiferromagnetism. *Phys. B+C* **1977**, *91*, 231–234. [[CrossRef](#)]
2. Stewart, G.R. Non-Fermi-liquid behavior in d- and f-electron metals. *Rev. Mod. Phys.* **2001**, *73*, 797–855. [[CrossRef](#)]
3. Umeo, K.; Kadomatsu, H.; Takabatake, T. Non-Fermi-liquid behaviour at the pressure-induced antiferromagnetic to nonmagnetic transition in a heavy-fermion compound, Ce<sub>7</sub>Ni<sub>3</sub>. *J. Phys. Condens. Matter.* **1996**, *8*, 9743–9757. [[CrossRef](#)]
4. Goltsev, A.V.; Abd-Elmeguid, M.M. Origin of the pressure dependence of the Kondo temperature in Ce- and Yb-based heavy-fermion compounds. *J. Phys. Condens. Matter.* **2005**, *17*, S813–S821. [[CrossRef](#)]
5. Löhneysen, H.V.; Rosch, A.; Vojta, M.; Wölfle, P. Fermi-liquid instabilities at magnetic quantum phase transitions. *Rev. Mod. Phys.* **2007**, *79*, 1015–1075. [[CrossRef](#)]
6. Pfleiderer, C. Superconducting phases of f-electron compounds. *Rev. Mod. Phys.* **2009**, *81*, 1551–1623. [[CrossRef](#)]
7. Ramirez, A.P. Strongly geometrically frustrated magnets. *Annu. Rev. Mater. Sci.* **1994**, *24*, 453–480. [[CrossRef](#)]
8. Lacroix, C.; Mendels, P.; Mila, F. *Introduction to Frustrated Magnetism*; Springer: Berlin/Heidelberg, Germany, 2011.
9. Dönni, A.; Ehlersz, G.; Maletta, H.; Fischeryk, P.; Kitazawa, H.; Zolliker, M. Geometrically frustrated magnetic structures of the heavy-fermion compound CePdAl studied by powder neutron diffraction. *J. Phys. Condens. Matter.* **1996**, *8*, 11213–11229. [[CrossRef](#)]
10. Kim, M.S.; Echizen, Y.; Umeo, K.; Kobayashi, S.; Sera, M.; Salamakha, P.S.; Sologub, O.L.; Takabatake, T.; Chen, X.; Sakakibara, T.T.T.; et al. Low-temperature anomalies in magnetic, transport, and thermal properties of single-crystal CeRhSn with valence fluctuations. *Phys. Rev. B* **2003**, *68*, 054416. [[CrossRef](#)]
11. Tokiwa, Y.; Stingl, C.; Kim, M.-S.; Takabatake, T.; Gegenwart, P. Characteristic signatures of quantum criticality driven by geometrical frustration. *Sci. Adv.* **2015**, *1*, e1500001. [[CrossRef](#)]
12. Tsuda, S.; Yang, C.L.; Shimura, Y.; Umeo, K.; Fukuoka, H.; Yamane, Y.; Onimaru, T.; Takabatake, T.; Kikugawa, N.; Terashima, T.; et al. Metamagnetic crossover in the quasikagome Ising Kondo-lattice compound CeIrSn. *Phys. Rev. B* **2018**, *98*, 155147. [[CrossRef](#)]
13. Kubo, H.; Umeo, K.; Katoh, K.; Ochiai, A.; Takabatake, T. Multiple Magnetic Transitions in a Frustrated Heavy-Fermion Antiferromagnet YbAgGe under Magnetic Field and Pressure. *J. Phys. Soc. Jpn.* **2010**, *79*, 064715. [[CrossRef](#)]
14. Oishi, R.; Ohmagari, Y.; Kusanose, Y.; Yamane, Y.; Umeo, K.; Shimura, Y.; Onimaru, T.; Takabatake, T. Heavy-Fermion Behavior in a Honeycomb Kondo Lattice CePt<sub>6</sub>Al<sub>3</sub>. *J. Phys. Soc. Jpn.* **2020**, *89*, 104705. [[CrossRef](#)]
15. Sahoo, J.; Flint, R. Symmetric spin liquids on the stuffed honeycomb lattice. *Phys. Rev. B* **2020**, *101*, 115103. [[CrossRef](#)]
16. Seifert, U.F.; Vojta, M. Theory of partial quantum disorder in the stuffed honeycomb Heisenberg antiferromagnet. *Phys. Rev. B* **2019**, *99*, 155156. [[CrossRef](#)]
17. Heying, B.; Rodewald, U.C.; Pöttgen, R.; Katoh, K.; Niide, Y.; Ochiai, A. Synthesis and Structure of YbCuGe and YbIrGe. *Mon. Chem.* **2005**, *136*, 655–661. [[CrossRef](#)]
18. Katoh, K.; Maeda, M.; Matsuda, S.; Ochiai, A. Crystal growth, magnetic and transport properties of single-crystal YbCuGe. *J. Alloys Compd.* **2012**, *520*, 122–126. [[CrossRef](#)]

19. Hayashi, K.; Umeo, K.; Takeuchi, T.; Kawabata, J.; Muro, Y.; Takabatake, T. Anisotropic dependence of the magnetic transition on uniaxial pressure in the Kondo semiconductors CeT<sub>2</sub>Al<sub>10</sub> (T = Ru and Os). *Phys. Rev. B* **2017**, *96*, 245130. [[CrossRef](#)]
20. Smith, T.F.; Chu, C.W.; Maple, M.B. Superconducting manometers for high pressure measurement at low temperature. *Cryogenics* **1969**, *9*, 53–58. [[CrossRef](#)]
21. Umeo, K. Alternating current calorimeter for specific heat capacity measurements at temperatures below 10 K and pressures up to 10 GPa. *Rev. Sci. Instrum.* **2016**, *87*, 063901. [[CrossRef](#)]
22. Umeo, K.; Igaue, T.; Chyono, H.; Echizen, Y.; Takabatake, T.; Kosaka, M.; Uwatoko, Y. Uniaxial-stress induced magnetic order in CeNiSn. *Phys. Rev. B* **1999**, *60*, R6957–R6960. [[CrossRef](#)]
23. Jennings, J.D.; Swenson, C.A. Effects of Pressure on the Superconducting Transition Temperatures of Sn, In, Ta, Tl, and Hg. *Phys. Rev.* **1958**, *112*, 31–43. [[CrossRef](#)]
24. Nakajima, T.; Mitsuda, S.; Takahashi, K.; Yoshimori, K.; Masuda, K.; Kaneko, C.; Honma, Y.; Kobayashi, S.; Kitazawa, H.; Kosaka, M.; et al. Uniaxial-Pressure Control of Magnetic Phase Transitions in a Frustrated Magnet CuFe<sub>1-x</sub>Ga<sub>x</sub>O<sub>2</sub> (x= 0, 0.018). *J. Phys. Soc. Jpn.* **2012**, *81*, 094710. [[CrossRef](#)]